JOURNAL OF CATALYSIS **161,** 605–613 (1996)
ARTICLE NO. 0223

Catalytic Properties of ZrO_2–SiO_2: Effects of Sulfation in the Cyclohexene Isomerization Reaction

J. A. Navío,[1] G. Colón, M. Macías, J. M. Campelo,* A. A. Romero,* and J. M. Marinas*

*Instituto de Ciencias de Materiales, Centro Mixto Universidad de Sevilla–CSIC, and Departamento de Química Inorgánica, Facultad de Química, Universidad de Sevilla, E-41012 Sevilla, Spain; and *Departamento de Química Orgánica, Facultad de Ciencias, Universidad de Córdoba, Avda. San Alberto Magno, s/n, E-14004 Córdoba, Spain*

Received July 20, 1995; revised October 16, 1995; accepted March 25, 1996

Catalytic properties of ZrO_2–SiO_2 (14% molar) for cyclohexene conversion (skeletal isomerization and hydrogen transfer) have been studied. Textural and morphological properties were correlated to explain catalytic behavior. XRD, DTA–TGA, N_2 adsorption, DRIFT, and acidity measurements by pyridine and dimethylpyridine chemisorption were used to characterize samples. The effect of the sulfation process upon surface structure as well on catalytic activity/selectivity has also been studied. It has been shown that catalytic activities are increased on sulfated samples, but at the same time products of the hydrogen transfer reaction seem to be increased too, lowering the selectivity of the reaction; isomerization always predominates. Sulfation transforms this compound to a relatively selective isomerization catalyst exhibiting greater catalytic activity.

INTRODUCTION

Zirconia, ZrO_2, is an important material that finds application in several fields. It has been reported that ZrO_2 shows specific catalytic activities for the cleavage of C–H bonds (1), the hydrogenation of 1,3-butadiene by molecular hydrogen and hydrogen donor molecules such as cyclohexadiene (2, 4), and high selectivities for the formation of 1-olefins from secondary alcohols (5) and isobutane in the reaction $CO + H_2$ (6). All this characteristic behavior of ZrO_2 is considered to be due to the acid–base bifunctional catalysis.

Other authors (7) have recently reported in detail on the properties of ZrO_2 supported silica using a variety of analytical procedures (XPS, SIMS, IR, TPD). They found that ZrO_2 on silica, when prepared form $Zr(OEt)_4$–acetic acid–methanol solution, have a far better ZrO_2 dispersion than similarly prepared derived from aqueos solutions. Also, the metal oxide dispersion of the ethoxide derived ZrO_2/SiO_2 was thermally (600–750°C) far more stable than the nitrate derived binary system. Maximizing the ZrO_2 dispersion is important since this probably enhances the catalyst's activity and selecivity (e.g., rate and efficiency), while the thermal stability of this dispersion is very important if the catalyst is to be regenerated by air burnoff (to remove nonvolatile organic deposits).

ZrO_2, in its tetragonal form, is stable above 1100–1200°C but not at room temperature (even when quenched). When ZrO_2 is dispersed on silica, this results in 50–150 Å crystallites. These have the tetragonal structure (8) and appear to be stable to 500°C. Another author (9) discussed the nature of "hydrous ZrO_2" (10) prepared by various precipitation techniques. This material is not monoclinic but cubic and stable to about 650°C.

We have shown (11, 12) that the physical and chemical properties of dispersed ZrO_2 on a SiO_2 matrix are different from those of bulk zirconia. Ishida *et al.* have recently reported (13) that superacid properties, which were obtained by well-dispersed ZrO_2 on a SiO_2 matrix, can be correlated with the extent of ZrO_2 crystallization.

Processed composites of x ZrO_2–(100–x) SiO_2 where the value of x ranges between 3 and 100% have been prepared. The textural properties of such samples have been widely studied by us (11). The surface behavior is noteworthy—the plot of specific surface area versus SiO_2 composition presents a "volcano" shape, with a maximum for $x = 14\%$ molar. This value rose in a later crystallization kinetic study of these samples (14). There is a limit in the crystallization model at 11.5% molar. This was shown again by XPS (15), where samples with a low content of ZrO_2 (<14% molar) showed no correspondence between EDAX analysis and XPS analysis of the surface composition.

In principle, these facts could lead us to assume that ZrO_2 coats SiO_2, forming a monolayer at an estimated value of 11.5% molar, approximately, with 14% being a composite with highest surface area and close to the monolayer behavior. However, previous results reported by us (11, 15) showed that the ZrO_2–SiO_2 composite with 14% molar of ZrO_2, really are constituted by SiO_2 particles partially coated of circonia and a small amount of individual SiO_2 and ZrO_2 particles.

In the present work we study the catalytic properties of ZrO_2–SiO_2 (14% molar) in the cyclohexene isomerization

[1] To whom correspondence should be addressed. Fax: 34-95-455 71 34.

0021-9517/96 $18.00

reaction. We study the effects of calcination temperature and sulfate groups on the acid sites distribution and catalytic yield for that reaction.

EXPERIMENTAL

Sample Preparation

Amorphous powders ZrO_2–SiO_2 (14% molar) were processed by a sol-gel chemical route. A solution of ammonia in deionized water was added dropwise with continuous stirring to a solution of $ZrOCl_2 \cdot 8H_2O$ (Fluka Chemika) containing silica gel (Aldrich, grade 634) as a core matrix in suspension. Details for the preparation can be found elsewhere (11). As previously mentioned, this method does not lead to a homogeneous system in wich ZrO_2 coats SiO_2 particles, in spite of that, the molar percent is close to the estimated value for the monolayer situation. These samples were then calcined at various temperatures (773, 873, and 1073 K) for 2 h. We called these samples ZS773, ZS873, and ZS1073, respectively. They were then submitted to a sulfation process. A certain amount of calcined sample was suspended in H_2SO_4 (1 N) solution at a rate of 3 ml per gram of catalyst and left for 1 h with continuous stirring to reach equilibrium. Sulfated samples were denominated ZS773S, ZS873S, and ZS1073S. (For textural studies sulfated samples were calcined at 773 K for 2 h to get exact information of surface at reaction conditions.)

Experimental Technique

Textural properties. Specific surface area and pore size were obtained from N_2 adsorption-desorption isotherms at 77 K, using a Micromeritics ASAP2000 analyzer. Pore size distribution was calculated using the Barrett, Joyner, and Halenda method, assuming cylindrical pore model (16).

DTA–TGA (differential thermal and thermogravimetric analysis) diagrams were obtained simultaneously in static air with a Setaram high-temperature thermal analyzer, Model 92-16, 18, at a heating rate of 8 K min^{-1}. Calcined alumina was used as reference material. A furnace of graphite heating element with alumina protection tube was used.

X-ray powder diffraction diagrams were obtained in a Siemens D-501 diffractometer, using Ni-filtered Cu $K\alpha$ radiation.

DRIFT and surface acidity. Spectra were recorded on an FTIR instrument (Bonem MB-100) equipped with diffuse reflectance (Spectra Tech, Collector). A resolution of 8 cm^{-1} with 256 scans was averaged to obtain a spectrum from 4000 to 400 cm^{-1}. KBr or nonsulfated samples were used as reference spectra.

Surface acidity was determined using pyridine (PY) and dimethylpyridine (DMPY) adsorption. Samples were previously heated at 573 K under dried N_2 for 1 h and then sequentially cooled to 473 and 373 K, the catalyst remaining 30 min at this temperature. PY and DMPY were then introduced by bubbling a stream of dehydrated and deoxygenated N_2 (20 ml min^{-1}) through the liquid (298 K) and into the sample chamber containing the neat catalyst sample at 373 K for 1 h. After 1 h of adsorption the system was flushed with N_2 to desorb the loosely bound PY, and DMPY from the surface of catalyst and the respective DRIFT were recorded. The samples were then heated in a N_2 stream to 473 and 573 K and the respective DRIFT spectra were obtained. Samples were equilibrated for at least 1 h at each temperature or reactant condition prior to spectra measurement.

Surface acidity (Lewis and Brønsted sites) was measured in a dynamic mode by means of the gas-phase (473–673 K) adsorption of PY and DMPY using a pulse chromatographic technique according to a method described elsewhere (13).

Catalytic reaction. Catalytic activity and selectivity for these samples in cyclohexene isomerization reaction was determined in a pulse microreactor (4 mm i.d.), with pulses of 1 μl of pure cyclohexene (supplied by Merck), connected to a gas chromatograph (HP 5890 II) with an FID detector using N_2 as carrier gas. A detailed description of the microreactor and the experimental procedure for measuring the catalytic activity have been given elsewhere (18). Reaction products were characterized by gas chromatography–mass spectrometry.

RESULTS AND DISCUSSIONS

Textural Properties

The DTA–TGA profile of ZrO_2–SiO_2 presents a single exothermic peak due to ZrO_2 crystallization, centered around 1173 K in this present sample (Fig. 1). So all the samples studied in this work might be amorphous. However, X-ray diffraction diagrams were made for all samples to ensure that the sulfation process and second heating treatment do not affect the ZrO_2 structure in any way, such as other authors have reported (19, 20).

X-ray diagrams for ZS1073, ZS1073 (recalcined at 773 K, 2 h), ZS1073S, and ZS1073S (recalcined at 773 K, 2 h) show amorphous patterns (Fig. 1) though with a certain short-range order, probably due to their calcination temperatures (1073 K) being close to the temperature of the crystallization peak. Thus, we conclude that all the samples, ZS773, ZS873, and ZS1073 and the corresponding sulfated samples, present no large-range rearrangement. Only these latter samples, shown in Fig. 1, present a certain short-range order but are still amorphous.

Specific surface areas were calculated by means of the n-method (S_n) and BET method (S_{BET}). As Table 1 shows, sol-gel prepared samples present high surface areas (in the

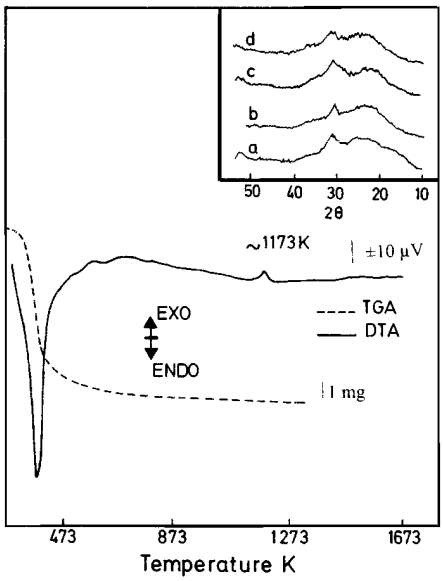

FIG. 1. DTA–TGA curve of ZrO_2–SiO_2 (14% molar) composite gel powders. XRD diagrams (Cu $K\alpha$ radiation) for: (a) ZS1073; (b) ZS1073 calcined 773 K, 2 h; (c) ZS1073S; (d) ZS1073S calcined 773 K, 2 h.

range 400–333 m^2/g). A slight decrease is observed in S_{BET} as the calcination temperature increases, although high surface areas remain.

For sulfated samples surface areas follow almost the same sequence, being in this case lower than for nonsulfated samples (possibly small pores collapsed after sulfate impregnation). There is no appreciable change in the pore volume (Fig. 2).

DRIFT Spectra

In Fig. 3 the spectra in the 4000–2500 cm^{-1} region are shown for the nonsulfated samples calcined at the indicated temperatures. As can be see, the IR spectrum of the ZS500 shows a sharp peak at 3740 cm^{-1} and more than one (broad) band at 3580 and 3350 cm^{-1}.

According to literature data (21, 22) the characteristic absorption band of the so-called isolated silanol groups (OH stretch mode of free single and geminal hydroxyls) is found

TABLE 1

Textural Properties of ZrO_2–SiO_2 (14% Molar) Catalysts

Catalyst	$S_{BET}/m^2\ g^{-1}$	$S_n/m^2\ g^{-1}$	$V_p/ml\ g^{-1}$	r_p/nm
ZS773	400	381	0.64	3.2
ZS873	351	336	0.65	3.7
ZS1073	333	316	0.56	3.4
ZS773S	321	305	0.53	3.3
ZS873S	315	301	0.63	4.0
ZS1073S	318	309	0.57	3.6

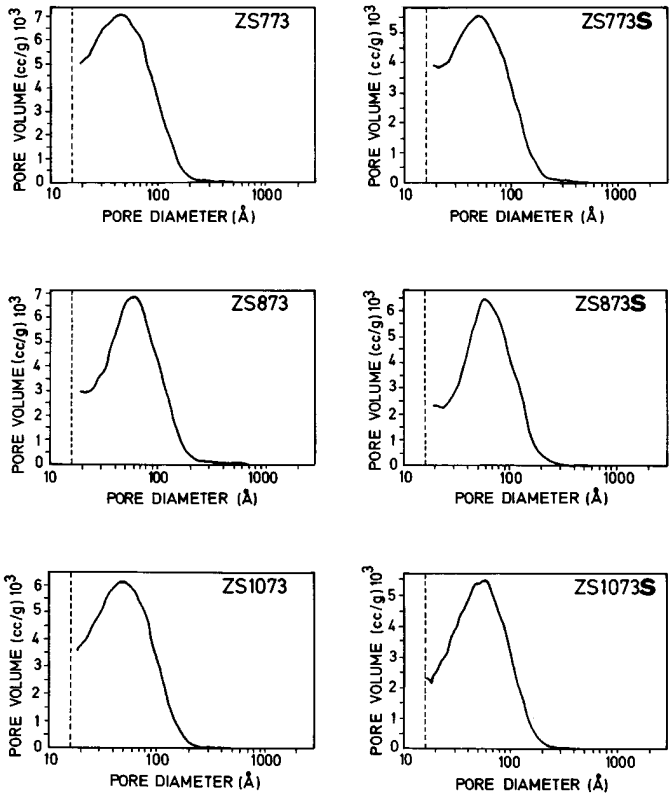

FIG. 2. Pore volume distribution for ZrO_2–SiO_2 (14% molar) samples.

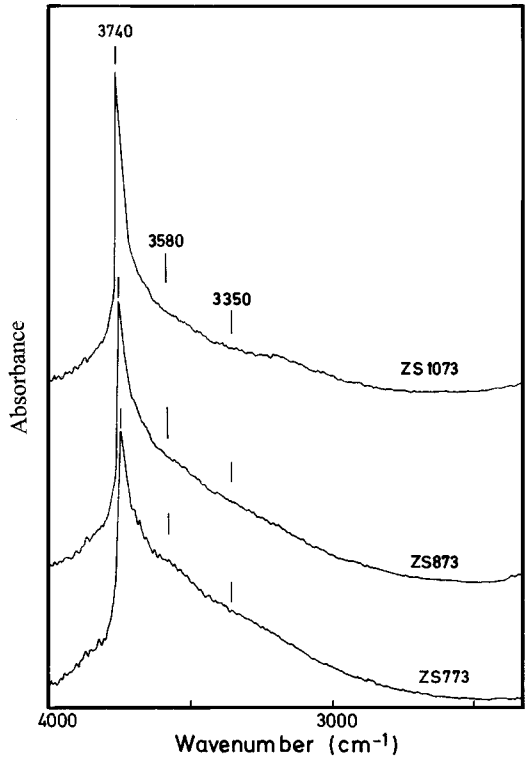

FIG. 3. DRIFT spectra of nonsulfated samples.

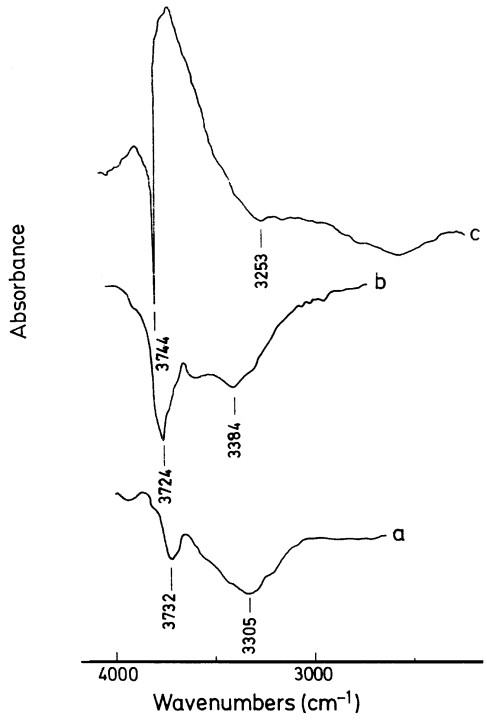

FIG. 4. DRIFT spectra of sulfated samples ratioed automatically against nonsulfated series. Negative peaks due to OH removal on ZrO_2–SiO_2 samples: (a) ZS773S; (b) ZS873S; (c) ZS1073S.

in silica and silica mixed oxides centered at 3740 cm^{-1}. Thus the peak at 3740 cm^{-1}, observed in the spectra of Fig. 3, must be assigned to OH stretch of isolated Si–OH.

On the other hand, the broad band at lower wavenumbers could be assigned to more than one type of OH groups in the mixed oxide, from different neighbor cations, depending on the Zr/Si ratio at the heterogeneous surface. It should be noticed that an increase in the calcination temperature remains practically unmodified the peak at 3470 cm^{-1}, while an appreciable decrease is observed at the lower wavenumber bands of this region. This results clearly indicate that calcination does not affect to the silanol groups.

Figure 4 shows the sulfated sample spectrum with nonsulfated subtracted, in the hydroxyl band frequency region. It shows the changes that appear after sulfation and recalcination at 773 K. Therefore, the decrease in this band may be due to a combined effect of sulfate attachment and later heating process at 773 K. The temperature effect could be understood as a sintering process for which hydroxyl groups can be removed, liberating water molecules. At the same time, the effect of sulfate produces a displacement of these hydroxyl groups, what combined with the thermal removing of the hydroxyl groups could lead to the collapse of the surface, as it is indicated in Scheme 1. The differential band centered around 3730 cm^{-1} can be assigned to terminal Si–OH removal and that at 3300–3380 cm^{-1} can be assigned to other different OH removal from the surface, mentioned before. As can be observed, the intensities of this second broad band is significantly lower than the 3730 cm^{-1} band. Due to the fact that the calcination does not affect the band at 3740 cm^{-1} as shown in Fig. 3, consequently the decrease in the intensity at the differential spectra (Fig. 4) can be associated to the effect of sulfate attachment instead of the recalcination process.

The differential spectra of the $SO_4^=$ region can be divided into two parts (Fig. 5). The first part, located around 1365 cm^{-1}, is due to $\nu_{S=O}$ (19, 20), and the second part, more complicated, corresponds to ν_{S-O}. The band centered at 1360 cm^{-1} may be assigned to isolated sulfates localized in the crystallographically defective configurations ($\nu_{S=O} < 1375$ cm^{-1} (20)).

Surface Acidity Measurements

The adsorption of probe molecules is widely used as direct measurement of surface acidity (24–29). PY and

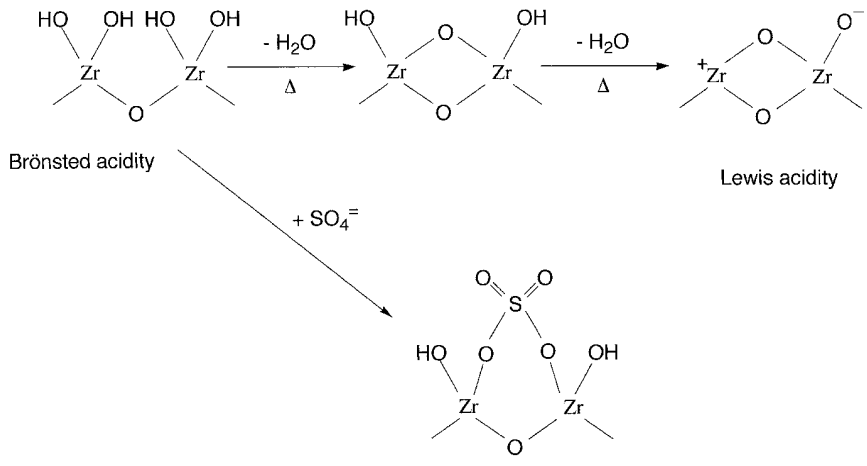

SCHEME 1

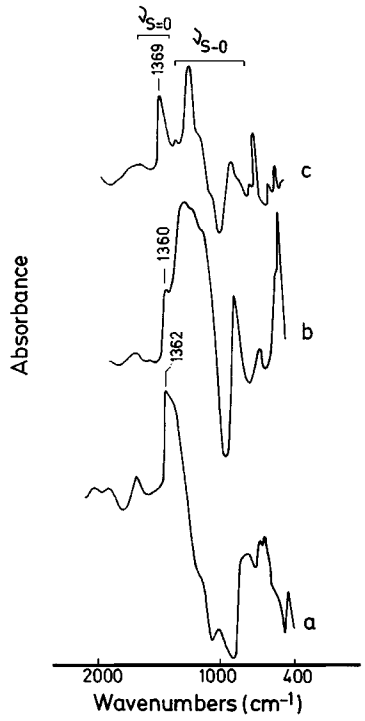

FIG. 5. DRIFT spectra of sulfated samples [(a) ZS773S; (b) ZS873S; (c) ZS1073S] showing $\nu_{S=O}$ and ν_{S-O} regions.

DMPY have been used in this study. They specifically adsorb on acid sites (Lewis and Brønsted).

Table 2 shows quantitative results of the adsorption of PY and DMPY. From PY adsorption, it is worth noting the sulfate effects. After sulfation treatment, the acid sites undergo a small decrease. Moreover, for sulfated samples the number of stronger acid sites is higher than for nonsulfated sites (56% for ZS773S vs 36% for ZS773). Therefore, sulfate groups not only modify the number of acid sites but also increase the strongest acid sites population by inductive effect (Structure 1). It can be observed that with calcination temperature, for all samples, acid sites are lost, remaining the strongest.

TABLE 2

Surface Acidity of ZrO_2–SiO_2 (14% Molar) Catalysts

Catalyst	PY/μmol g^{-1} 573 K	PY/μmol g^{-1} 673 K	DMPY/μmol g^{-1} 673 K
ZS773	87	32 (36%)[a]	6
ZS873	76	24 (31%)	13
ZS1073	52	26 (50%)	3
ZS773S	62	35 (56%)	43
ZS873S	59	53 (89%)	38
ZS1073S	51	39 (76%)	20

[a] Percentage of acid site present after evacuation at 673 K respect to initial population at 573 K.

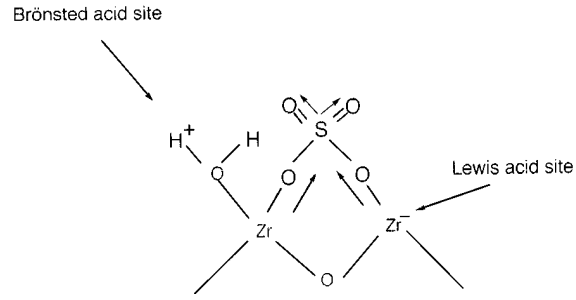

STRUCTURE 1

From the DMPY adsorption results, it can be observed that the number of Brønsted acid sites is significantly greater for sulfated samples. Calcination temperature affects Brønsted acid sites population (Scheme 1). Thus for sulfated samples Brønsted sites decrease gradually, being always greater than for nonsulfated samples. Sulfate groups are linked to Brønsted acid sites which become fewer after calcination. However, this weakens the O–H bond and therefore strengthens the acidity of remaining hydroxy groups (Structure 1).

Pyridinium is adsorbed on Brønsted sites, forming pyridinium ion (1535–1550 and 1640 cm^{-1}, approx.). PY is adsorbed on Lewis sites, by donation of the lone electron pair of nitrogen to the acid site (σ donation to a coordinatively unsaturated cation, 1447–1464 cm^{-1}) (24–26). The predominant band that characterizes Lewis acid sites is located at 1451 cm^{-1}, while 1544 cm^{-1} is the characteristic band for Brønsted acid sites. On the other hand, Uytterhoeven *et al.* have reported (27) that the 1493 cm^{-1} band corresponds to the Brønsted and Lewis chemisorption. So we must examine those bands to correlate the acid center behavior. DMPY is specifically adsorbed on Brønsted sites due to a steric effect, and due to its higher basic strength it will detect the weakest acid centers (28) with bands located at 1628 and 1648 cm^{-1} for Brønsted sites and 1465 and 1580 cm^{-1} for Lewis sites (29).

After PY adsorption in nonsulfated samples bands appeared at 1647 cm^{-1} (B), 1601 cm^{-1} (L), 1.574 cm^{-1} and 1547 cm^{-1} (B), and 1489 cm^{-1} (B + L), and 1447 cm^{-1} (L) (Fig. 6A); these latter ones are very intense. Increasing temperature and times of adsorption most affected bands located at 1447 and 1489 cm^{-1} (Fig. 6A)—in other words, Lewis acid sites. That is, Brønsted sites are stronger than Lewis sites. Figure 7A shows spectra for sulfated samples. In this case the bands assigned to Brønsted sites appear with higher intensities. The presence of bands at 573 K/60 min suggest that these Brønsted sites also appear with higher acid strength.

With respect to DMPY adsorption (Figs. 6B and 7B), bands are observed at 1640 cm^{-1} (B), 1601 cm^{-1} (L), 1582 cm^{-1} (L), and 1462 cm^{-1} (L). Bands centered at 1601 and 1582 cm^{-1} disappear, giving a broad band of low

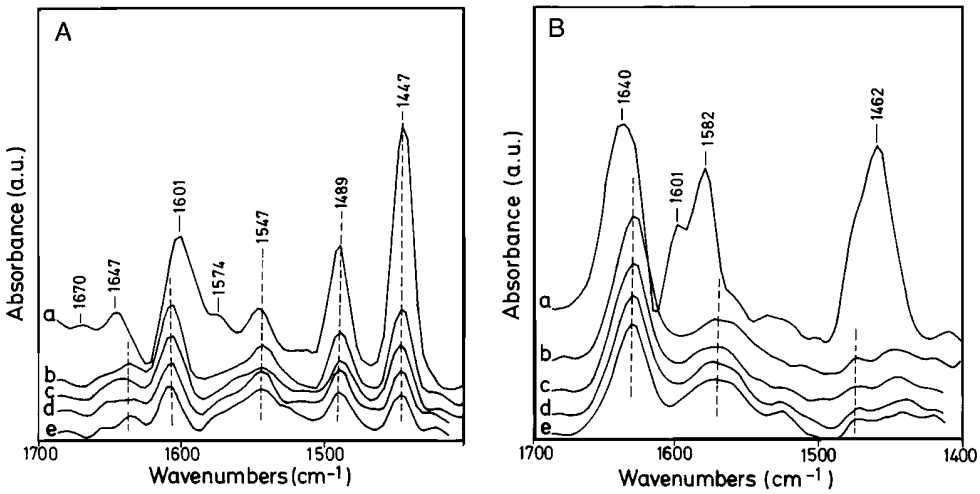

FIG. 6. DRIFT spectra of (A) PY and (B) DMPY on ZS773 sample. The sample was dried at 573 K under N_2, cooled to 373 K, and then loaded with PY or DMPY and flushed with N_2 for 30 min (a). The temperature was then increased to 473 K and the catalyst remained, in N_2 stream, at 473 K for 30 min (b); 1 h (c); 2 h (d); and 3 h (e).

intensity located around 1560 cm^{-1} . At the same time the 1640 cm^{-1} band decreases to lower wavenumbers.

Sulfated samples (Fig. 7B) present DMPY adsorption bands centered at 1636 cm^{-1}, 1582 cm^{-1} (with a shoulder at 1600 cm^{-1}), and 1462 cm^{-1}. Only the 1636 cm^{-1} band remains on increasing temperature and times of adsorption, located finally at lower wavenumbers (Fig. 7B) and with higher intensity than in nonsulfated samples.

Catalytic Study

The cyclohexene (CHE) isomerization reaction (cyclohexene skeletal isomerization, CSI) was used as catalytic test for these catalysts, due to its capability in characterizing the acid strength of protonic sites (30). The reaction path is shown in Scheme 2.

The catalytic runs have been carried out in the absence of diffusional influences (boundary layer, internal, and external mass transfer process) through the choice of the suitable operating variables, specifically space velocity (changing the catalyst weight and the carrier gas flow) and particle size (below 0.7 mm); furthermore, the amount of catalyst corresponded to similar area loaded in the reactor. The catalytic runs have also been carried out at different weight ratios of catalyst from the cyclohexene introduced, showing

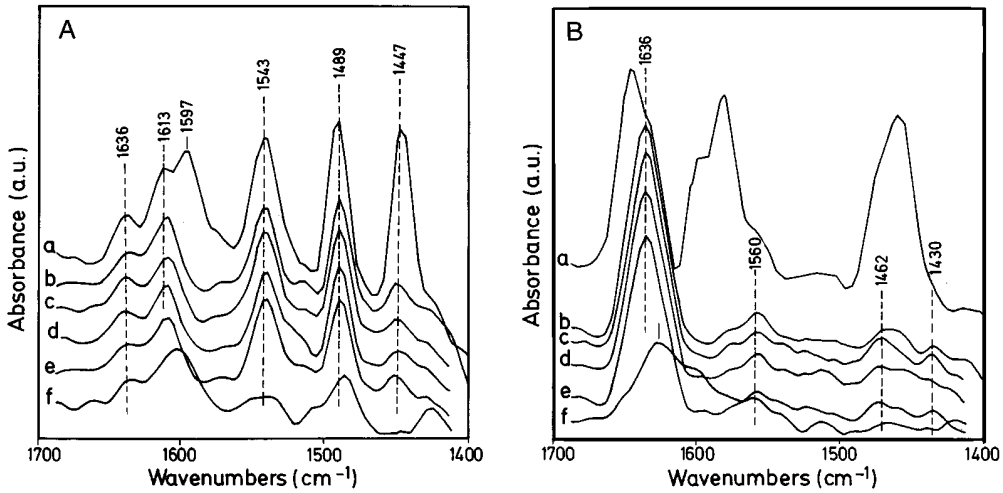

FIG. 7. DRIFT spectra of (A) PY and (B) DMPY on ZS773S sample. The sample was dried at 573 K under N_2, cooled to 373 K, and then loaded with PY or DMPY and flushed with N_2 for 30 min (a). The temperature was then increased to 473 K and the catalyst remained, in N_2 stream, at 473 K for 30 min (b); 1 h (c); 2 h (d); and 3 h (e); and finally at 573 K for 1 h (f).

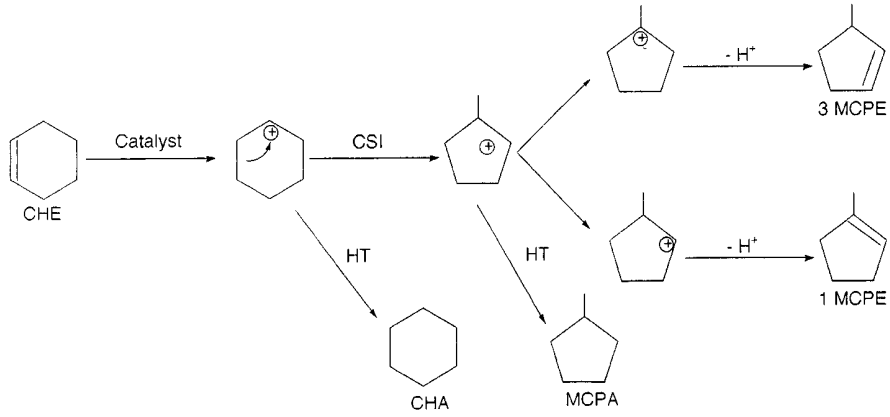

SCHEME 2

that the fractional conversion of reactant to products was independent of the pressure, which determined the first-order reaction process. This behavior also ensured linear chromatography in the pulse mode, i.e., ensuring equilibrium chromatography.

In the absence of mass transfer process, the conversion of cyclohexene (which was maintained below 20% level) followed the requirement of Bassett–Habgood kinetic treatment (31) for the first-order kinetic process in which the rate determining step is the surface reaction:

$$\ln[1/(1-X)] = \mathrm{RT}K_a(W/F), \qquad [1]$$

where X is the conversion, K_a is the aparent rate constant of the surface process, W is the catalyst weight, and F is the flow rate of carrier gas.

The $\ln[1/(1-X)]$ vs F^{-1} plots according to Eq. [1], for the conversion of cyclohexene at various flow rates of the nitrogen carrier gas (20–40 ml $\cdot$ min^{-1}) and different reaction temperatures are linear and also pass through the origin, indicating a good fit of the data to Eq. [1] and, therefore, the first-order process in the cyclohexene conversion.

As reaction products for cyclohexene isomerization, 1- and 3-methylcyclopentene (1-MCPE and 3-MCPE respectively) can be obtained, 1-MCPE being the main product. The hydrogen transfer reaction (HT) also appears as a competitive reaction, giving as secondary products cyclohexane (CHA) and methylcyclopentane (MCPA) (see Scheme 2).

Table 3 shows activation and kinetic data for the isomerization reaction of cyclohexene (CSI). The apparent rate constant K_a at 523 K gives direct measurement of the degree of reaction. Activation parameters (E_a and ln A) have been obtained by the Arrhenius equation; experimental selectivities (S_{CSI}) are also included in Table 3. Table 4 contains the same variables for HT.

Position of the 98% confidence limit lines and the value of the coefficient of determination (always over 0.99) for the regressions are used to check the adequacy of the data. A Student's t test of significance showed that those are significant levels over 1%. At least three measurements where used to calculate each value of K_a. All values are reproducible to within about 7%.

For nonsulfated samples it is worth noting that K_a for CSI decreases drastically with calcination temperature, having its lowest value at 873 K. In contrast, sulfated samples experiment a great increase, without too much difference between samples.

There is a great controversy about the nature of the promoter for the acid–base catalytic activity (23, 32). We observe that K_a depends on the presence of S=O groups rather than on the calcination process. As previously mentioned, the incorporation of sulfate ions on these samples enhances the acidic strength of the remaining hydroxy groups and consequently this effect may lead to an increase in the catalytic activity for CSI as is readily observed.

For the HT reaction, lower K_a values are observed for both nonsulfated and sulfated samples, with the same tendency—a gradual but considerable decrease with temperature.

OPE (optimum performance envelope) curves (33, 34) that show the product distribution in the reaction for each

TABLE 3

Aparent Rate Constant (K_a), Activation Parameters (E_a, ln A), and Experimental Selectivities (S_{CSI}) for CSI on ZrO_2–SiO_2 (14% Molar) Catalysts

Catalyst	$K_a/10^6$ [a] (mol atm^{-1} g^{-1} s^{-1})	E_a/kJ mol^{-1}	ln A	S_{CSI}
ZS773	42.9	52.3	2.0	85.9
ZS873	3.1	80.7	5.9	86.5
ZS1073	6.6	52.5	1.1	64.1
ZS773S	518.1	32.6	−5.7	66.4
ZS873S	465.1	42.9	2.2	84.3
ZS1073S	411.4	37.9	1.0	85.5

[a] At reaction temperature of 523 K.

TABLE 4

Aparent Rate Constant (K_a), Activation Parameters (E_a, ln A), and Experimental Selectivities (S_{HT}) for HT on ZrO_2–SiO_2 (14% Molar) Catalysts

Catalyst	$K_a/10^6$ [a] (mol atm^{-1} g^{-1} s^{-1})	E_a/kJ mol^{-1}	ln A	S_{HT}
ZS773	6.9	36.8	−3.4	14.1
ZS873	0.5	59.3	−0.9	13.4
ZS1073	3.7	33.3	−10.2	35.9
ZS773S	228.1	26.7	−2.2	33.5
ZS873S	77.0	19.0	−5.1	15.7
ZS1073S	48.7	23.5	−4.2	14.5

[a] At reaction temperature of 523 K.

total conversion (X_T molar%) have been plotted. From these plots the following results may be pointed out. Conversions for the first series of samples are relatively low (from 14 to 9%, lowest value for ZS873, 4%), the main product being 1-MCPE (75% with respect to 3-MCPE). HT is more outstanding in CHE than in isomerization products since MCPA is produced in a very low percentage. For ZS873 there is a deactivation at pulses beyond 523 K.

In the sulfated samples, conversions are much higher (about 40% for ZS773S and with a minimum using ZS873S, 24%). In this case HT for ZS773S is considerably higher, in the sense that CSI takes place to 66%; a great amount of MCPA is observed (Fig. 8). In other words, hydrogenation is important for the products of the isomerization reaction (1- and 3-MCPE), but not for the reagent (CHE).

For ZS873S and ZS1073S the CSI reaction appears with 83 and 85%, respectively, versus HT, but again MCPA has molar percentages higher than for nonsulfated samples. The deactivation process is important for these samples, taking place in pulses at above 323 K. It is worth noting that sulfated samples are more reactive than nonsulfated samples but with low selectivity for CSI, the products of HT appearing in even greater amount than 3-MCPE for ZS773S. In this sense, ZS1073S presents the most activity and selectivity for cyclohexene isomerization to 1-MCPE.

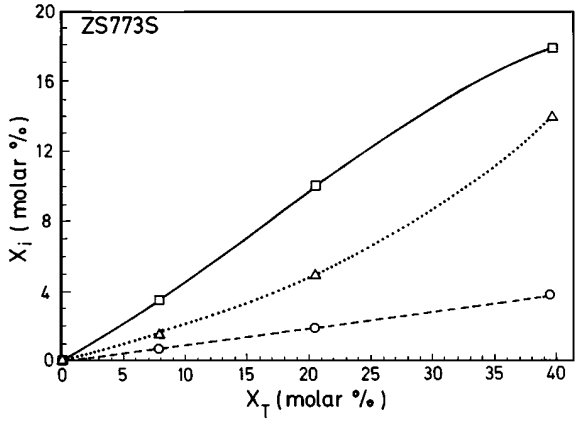

FIG. 8. OPE curve for [(□) $X_{1\text{-MCPE}}$, (○) $X_{3\text{-MCPE}}$, and (△) X_{MCPA} vs X_T] ZS773S sample.

CONCLUSIONS

ZrO_2–SiO_2 (14% molar) has been used as isomerization catalyst. The effect of calcination temperature and the presence of sulfate groups on the catalyst surface have been studied.

The presence of sulfate groups enhances the surface acidity, especially Brønsted acid sites possibly responsible for catalytic activity. Though there is great controversy on the origin of the catalytic activity, we have shown that for ZrO_2–SiO_2 samples studied here, the sites responsible for the increasing activity in the isomerization reaction are Brønsted acid sites, as can be inferred from PY and DMPY chemisorption studies and relative catalytic tests.

It has been shown that the sulfation process on different calcined samples has no marked effect on textural properties (S_{BET}, pore distribution) but has so on acidic properties—as much in the type of acid sites as in the strength of these sites. Surface acidity is a direct cause of catalytic activity. For cyclohexene isomerization, the calcination temperature has no great effect on catalytic activity. Thus conversions and selectivities vary over a short range, always being a minimum for ZS873.

For sulfated samples, conversions and selectivity have considerable variations. Conversions are in all cases greater than for nonsulfated samples and the selectivity decreases due to the hydrogenation reaction that takes place with isomerization products (more important in ZS773S). In particular, sample ZS1073S seems to be the most active and selective for CSI to 1-MCPE.

ACKNOWLEDGMENTS

The authors acknowledge financial support by a NATO grant (HTECH. CRG 931258, 1993) and financial support from the "Dirección General de Investigación Científica y Técnica" (DGICYT), Projects PB92-0816 and PB93-0917.

REFERENCES

1. Yamaguchi, T., Nakano, Y., Iizuka, T., and Tanabe, K., *Chem. Lett.* 1053 (1976).
2. Yamaguchi, T., and Hightower, J. W., *J. Am. Chem. Soc.* **99**, 4201 (1977).
3. Nakano, Y., Yamaguchi, T., and Tanabe, K., *J. Catal.* **80**, 307 (1983).
4. Shima, H., and Yamaguchi, T., *J. Catal.* **90**, 160 (1984).
5. Yamaguchi, T., Sasaki, H., and Tanabe, K., *Chem. Lett.* 1017 (1973).
6. Maruya, K., Inaba, A., Maehashi, T., Domen, T., and Onishi, T., *J. Chem. Soc. Faraday Trans. I* **77**, 2815 (1981).
7. Meijers, A. C. Q. M., de Jong, A. M., van Gruijthuijsen, L. M. P., and Niemantsverdriet, J. W., *Appl. Catal.* **70**, 53 (1991).
8. Gravie, R. C., *J. Phys. Chem.* **69**, 1238 (1965).
9. Clearfield, A., *Inorg. Chem.* **3**, 146 (1964).

10. Yamaguchi, T., Morita, T., Salama, T. M., and Tanabe, K., *Catal. Lett.* **4**, 1 (1990).
11. Navío, J. A., Marchena, J. F., Macías, M., and Sánchez-Soto, P. J., *in* "Ceramics Today—Tomorrow's Ceramics" (P. Vincenzini, Ed.) Materials Science Monographs, Vol. 66b, p. 889. Elsevier, Amsterdam, 1990.
12. Navío, J. A., Macías, M., Colón, G., and Sánchez-Soto, P. J., *Appl. Surf. Sci.* **70/71**, 226 (1994).
13. Ishida, T., Yamaguchi, T., and Tanabe, K., *Chem. Lett.* 1869 (1988).
14. Sánchez-Soto, P. J., Macías, M., Avilés, M. A., Colón, G., and Navío, J. A., *J. Sol Gel Sci. Technol.* **2**, 353 (1994).
15. Navío, J. A., Macías, M., Colón, G., Sánchez-Soto, P. J., Augugliaro, V., and Palmisano, L., *Appl. Surf. Sci.* **81**, 325 (1994).
16. Barrett, E. P., Joyner, L. S., and Halenda, P. P., *J. Am. Chem. Soc.* **73**, 373 (1951).
17. Bautista, F. M., Campelo, J. M., García, A., Luna, D., Marinas, J. M., and Romero, A. A., *Appl. Catal.* **104**, 109 (1993).
18. Campelo, J. M., García, A., Luna, D., Marinas, J. M., and Martinez, M. I., *Mater. Chem. Phys.* **21**, 409 (1989).
19. Morterra, C., Cerrato, G., Emanuel, C., and Bolis, V., *J. Catal.* **142**, 349 (1993).
20. Morterra, C., Cerrato, G., and Bolis, V., *Catal. Today* **17**, 505 (1993).
21. Niwa, M., Katada, N., and Murakami, Y., *J. Catal.* **134**, 340 (1992).
22. Odenbrand, C. U. I., Andersson, S. L. T., Andersson, L. A. H., Brandin, J. G. M., and Busca, G., *J. Catal.* **125**, 541 (1990).
23. Davis, B. H., Keogh, R. A., and Srinivasan, R., *Catal. Today* **20**, 219 (1994).
24. Knozinger, H., *Adv. Catal.* **25**, 184 (1976).
25. Parry, E. P., *J. Catal.* **2**, 371 (1963).
26. Basila, M. R., Kantner, T. B., and Rhee, K. H., *J. Phys. Chem.* **68**, 3197 (1964).
27. Uytterhoeven, J. B., Schonheydt, R., Liengme, B. V., and Hall, W. K., *J. Catal.* **13**, 425 (1969).
28. (a) Corma, A., Rodellas, C., and Fornés, V., *J. Catal.* **88**, 374 (1984); (b) Benesi, H. A., *J. Catal.* **28**, 76 (1973).
29. Jacobs, P. A., and Heydn, C. F., *J. Catal.* **34**, 267 (1973).
30. Blanco, A., Campelo, J. M., García, A., Luna, D., Marinas, J. M., and Moreno, M. S., *Appl. Catal.* **53**, 135 (1989).
31. Bassett, D., and Habgood, H. W., *J. Phys. Chem.* **64**, 769 (1960).
32. Comellí, R. A., Vera, C. R., and Parera, J. M., *J. Catal.* **151**, 96 (1995).
33. Best, D., and Woijciechowski, H. W., *J. Catal.* **47**, 11 (1977).
34. Ko, A. N., and Woijciechowski, H. W., *Int. J. Chem. Kinet.* **15**, 1249 (1983).